## Supporting Information

**Materials** All the reagents used were of analytical grade without further purification. Poly(ethyleneimine) (PEI, MW 750000) and Poly(sodium-p-styrenesulfonate) ( PSS, MW 70000) were purchased from Aldrich and were used without further treatment. Other chemicals were analytical grade without further purification. Water was purified using a Millipore Milli-Q water purification system.

**Instrumentation** A CHI 660C electrochemical workstation was used for all the electrochemical experiments. It combined with a Varian Cary 50 UV-vis spectrophotometer (Simadzu Co., Japan) to construct an in-situ spectroelectrochemical system for the electrochromic response measurement and with a Horiba Jobin Yvon Fluorolog-3 Spectrofluorometer to construct an in-situ fluorescence spectroelectrochemical system for the electroswitchable fluorescence response measurement, respectively.

**Preparation** The substrates, ITO-coated glass, were cleaned according to literature, the multilayer films were fabricated according to an electrostatic LBL technique.[17] In a typical process, the cleaned substrate was pretreated in a PEI aqueous solution (0.1g/ml pH =4.8 adjusted by 1M HCl) for 20 min to make the surface positively charged. Then the PEI-coated substrate was dipped into a $P_5W_{30}$ aqueous solution (2 mM) for 20 min, followed by rinsing with copious water and drying under nitrogen flow. Then the substrate was immersed into the PEI aqueous solution for 20 min and washed extensively with water. Then the substrate was immersed into the GO@F[18] (0.1 g/ml) aqueous solution for 20 min and washed extensively with water. The

multilayer films were successfully fabricated by alternate immersion of the substrates into different aqueous solution for many cycles.

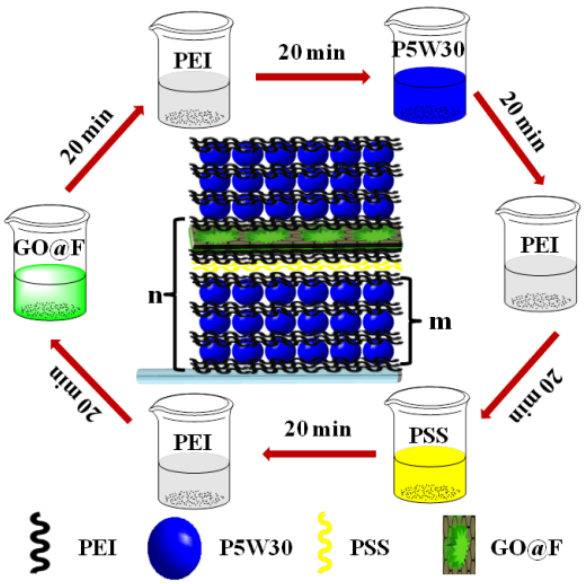


**Scheme 1.** Fabrication illustration of three hybrid films {[(PEI/$P_5W_{30}$)m/(PEI/PSS/PEI/GO@F)]n(PEI/$P_5W_{30}$)m} (m = 1, 3, 5; n = 15, 17, 18) on the ITO coated glass substrates.

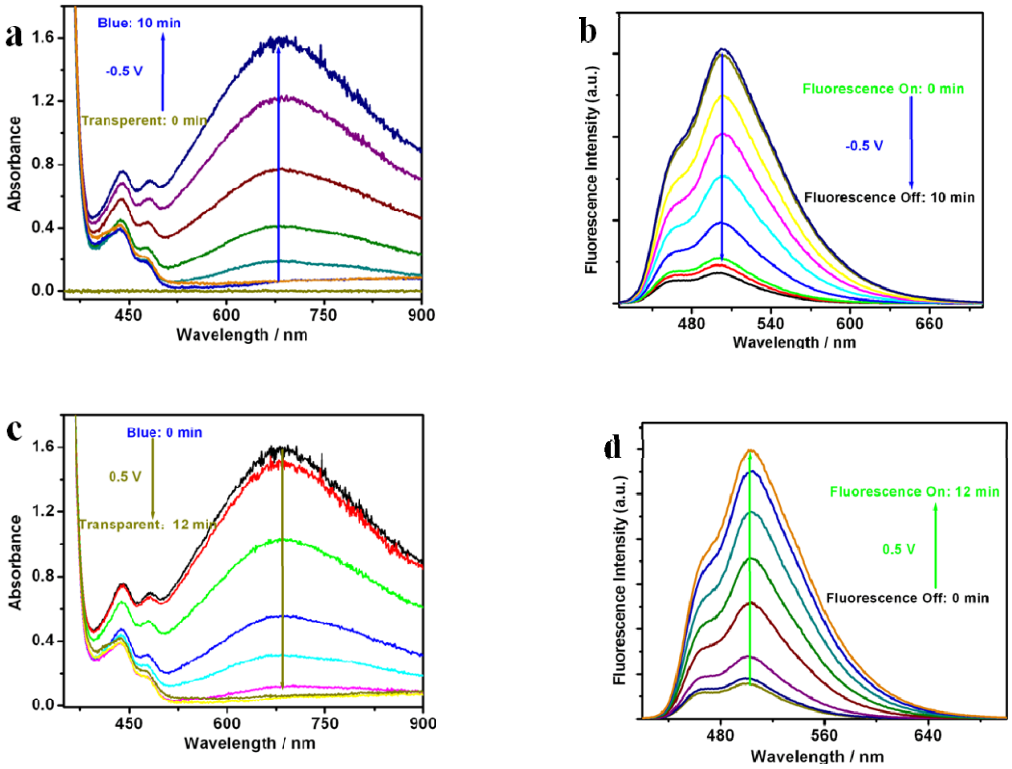


**Fig. S1** Absorption spectra in visible region 400 – 800 nm and luminescence spectra of $P_5W_{30}$ and F mixtures in pH 2.5 buffer solutions: **(a)** the absorbances increase as reduction time increasing 0-10min; **(b)** the fluorescence intensities decrease as reduction time increasing 0-10min; **(c)** the absorbances decrease as oxidation time increasing 0-12min; **(d)** the fluorescence intensities increase as oxidation time increasing 0-12min.

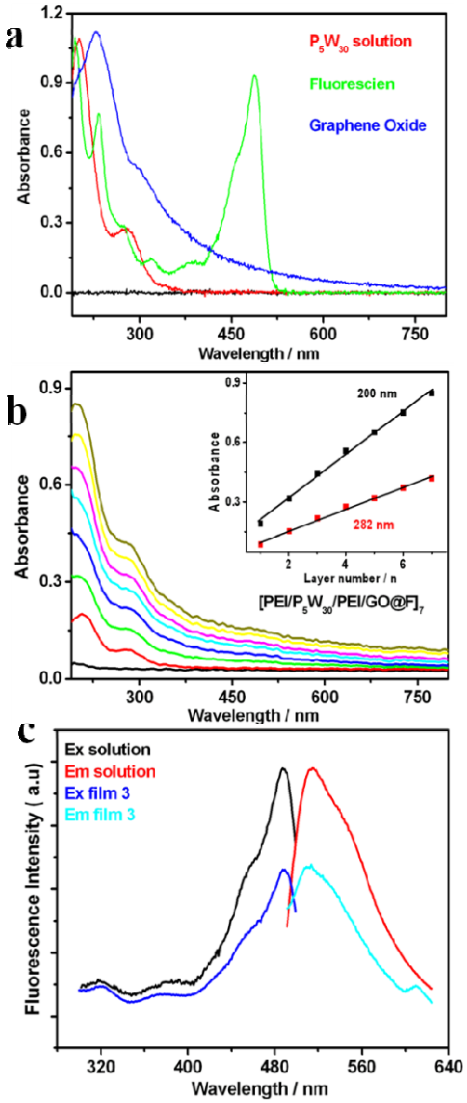


**Fig. S2** (a) UV-Vis absorption spectra of $P_5W_{30}$, GO and F in aqueous solutions and (b) UV-Vis absorption spectra of $[PEI/P_5W_{30}/PEI/GO@F]_7$ hybrid film, the inset shows the absorbances at 200 nm and 282 nm vs. the number of layers. (c) Excitation spectra of fluorescein solution (black line) and the hybrid film (blue line) at 507 nm, and emission spectra of fluorescein solution (red line) and the hybrid film (cyan line) at 485 nm.

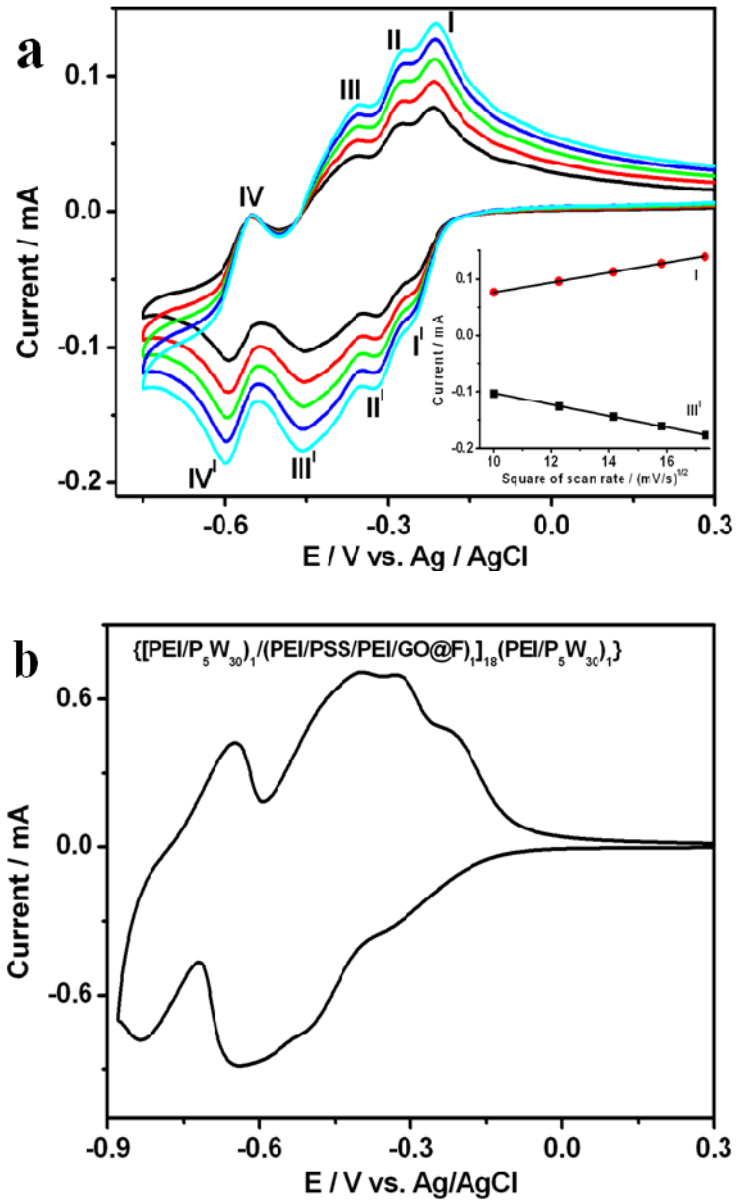


**Fig. S3** (a) CVs of 2 mM $P_5W_{30}$ in 0.5M $H_2SO_4/Na_2SO_4$ buffer solution with different scan rates: 100, 150, 200, 250, 300 $mVs^{-1}$, the inset shows the relationship of peaks I and II' vs. the square of scan rates; (b) CV of ITO electrode coated with $\{[(PEI/P_5W_{30})_1/(PEI/PSS/PEI/GO@F)_1]_{18}/(PEI/P_5W_{30})_1\}$ multilayer film in 0.5M $H_2SO_4/Na_2SO_4$ buffer solution (pH = 2.5) with a scan rate of 100 $mV \cdot s^{-1}$.

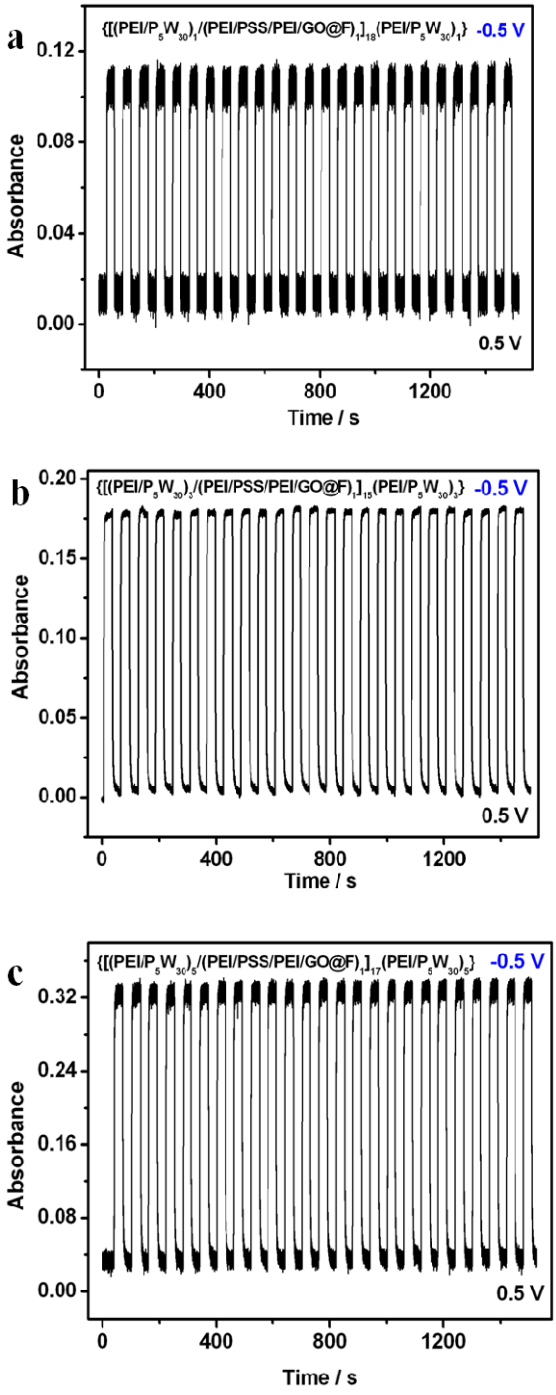


**Fig. S4** Absorbance at 650 nm of three hybrid films (a) $\{[(PEI/P_5W_{30})_1/(PEI/PSS/PEI/GO@F)_1]_{18}/(PEI/P_5W_{30})_1\}$, (b) (b)$\{[(PEI/P_5W_{30})_3/(PEI/PSS/PEI/GO@F)_1]_{15}/(PEI/P_5W_{30})_3\}$, (c) $\{[(PEI/P_5W_{30})_5/(PEI/PSS/PEI/GO@F)_1]_{17}/(PEI/P_5W_{30})_5\}$ on ITO-coated glass slides during subsequent double-potential steps from -0.5 to 0.5 V in 0.5M $H_2SO_4$+$Na_2SO_4$ solutions (pH = 2.5).

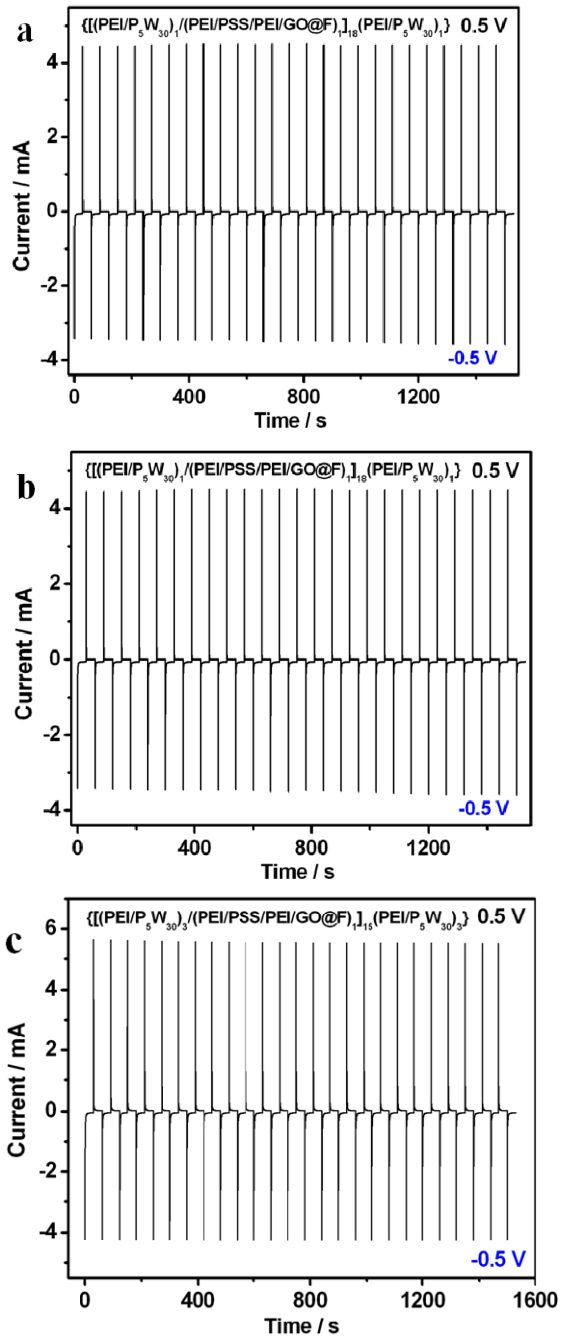


**Fig. S5** Currents of three hybrid films (a) $\{[(PEI/P_5W_{30})_1/(PEI/PSS/PEI/GO@F)_1]_{18}/(PEI/P_5W_{30})_1\}$, (b) $\{[(PEI/P_5W_{30})_3/(PEI/PSS/PEI/GO@F)_1]_{15}/(PEI/P_5W_{30})_3\}$, (c) $\{[(PEI/P_5W_{30})_5/(PEI/PSS/PEI/GO@F)_1]_{17}/(PEI/P_5W_{30})_5\}$ on ITO-coated glass slides during subsequent double-potential steps from -0.5 to 0.5 V in 0.5M $H_2SO_4$+$Na_2SO_4$ solutions (pH = 2.5).

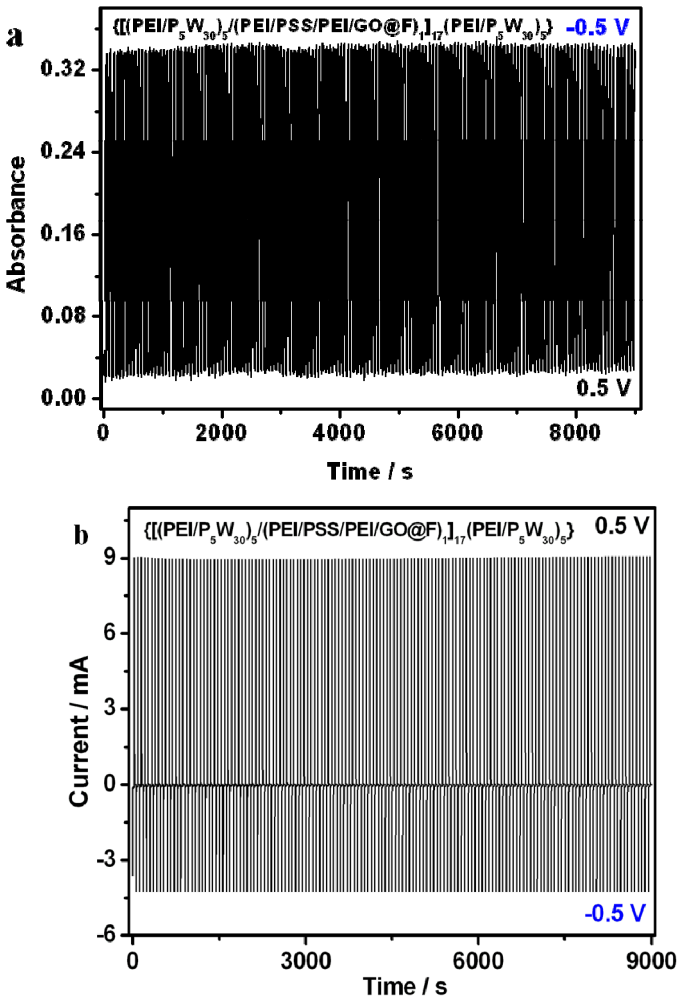


**Fig. S6** (a) Absorbance at 650 nm and (b) currents of the hybrid film $\{[(PEI/P_5W_{30})_5/(PEI/PSS/PEI/GO@F)_1]_{17}/(PEI/P_5W_{30})_5\}$ on an ITO-coated glass slide during subsequent double-potential steps from -0.5 to 0.5 V in 0.5 M $H_2SO_4$+$Na_2SO_4$ solution (pH = 2.5).

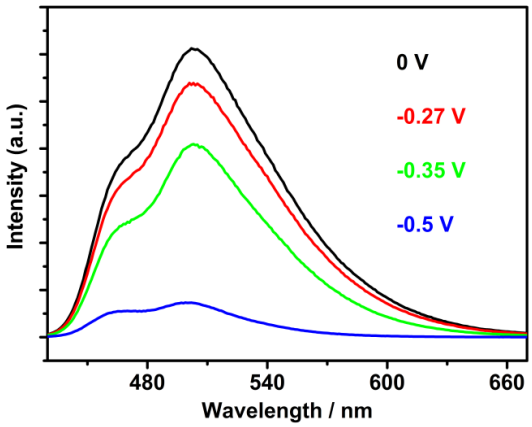


**Fig. S7**. Luminescence spectra of $P_5W_{30}$ (1mM) and F (2.66μM) mixtures in 0.5 M $Na_2SO_4$ + $H_2SO_4$ (pH 2.5) under open circuit (black curve) and electrochemical reduction at the different applied potentials of -0.27 V (red curve), -0.35V (green curve) and -0.5V (blue curve) for 30 min.

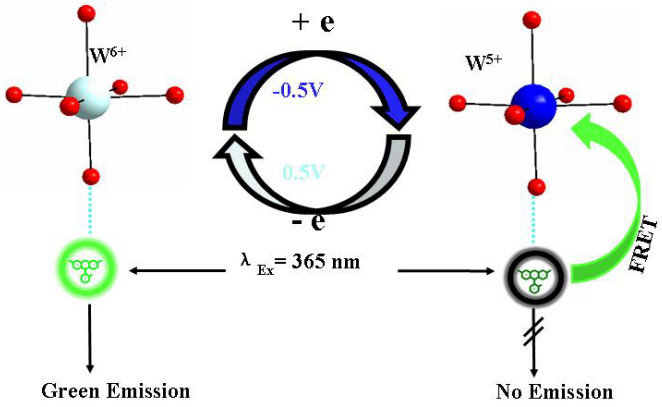


**FRET：Fluorescence Resonant Energy Transfer**

**Fig. S8.** Electrochemically induced fluorescence switch illustration of the system containing F and $P_5W_{30}$

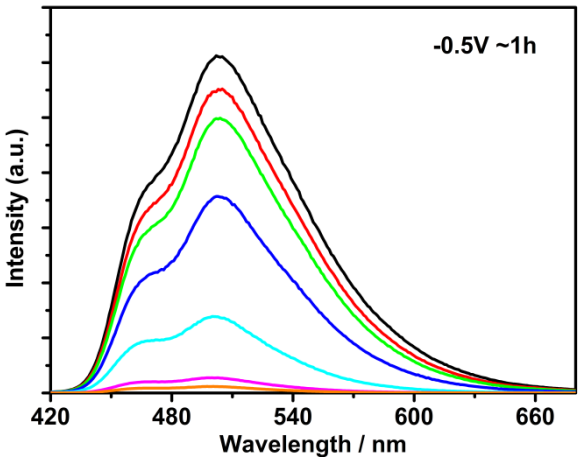


**Fig. S9**. Luminescence spectra of 2.66μM F in 0.5 M $Na_2SO_4$ + $H_2SO_4$ (pH 2.5) under open circuit (black curve) and electrochemical reduction at the applied potential of -0.5V for 1h at the different concentrations of $P_5W_{30}$ of 0.2 (red curve), 0.4 (green curve), 0.6 (blue curve), 0.8 (cyan curve), 1.0 (purple curve) and 1.2 mM (orange curve) with the ratio of C($P_5W_{30}$):C(F) = 75, 150, 225, 300, 375, 450, respectively.

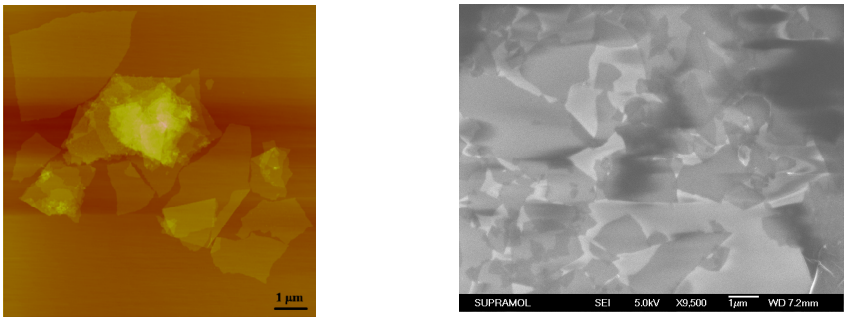


**Fig. S10**. AFM (left) and SEM (right) images of graphene oxide.

The surface morphology of the composite films has been characterized by AFM and SEM images.

**Fig. S11** shows typical AFM and SEM images of the composite films of $[PEI/P_5W_{30}]_1$ (A), $[PEI/P_5W_{30}/PEI/GO@F]_1$ (B), $[PEI/P_5W_{30}]_3$ (C), $[PEI/P_5W_{30}]_3[PEI/GO@F]$ (D), $[PEI/P_5W_{30}/PEI/F@GO]_3[PEI/P_5W_{30}]_1$ (E), $[PEI/P_5W_{30}/PEI/F@GO]_4$ (F). It can be seen that the composite films of A, C and E with $P_5W_{30}$ as the outermost layer showed the particles of $P_5W_{30}$ clusters adsorbed on PEI chains, while the composite films of B, D and F with GO@F as the outermost layer displayed the silk-like morphology, indicating that the surface morphology of the composite films with $P_5W_{30}$ as the outermost layer is significantly different from that of the composite films with GO@F as the outermost layer.

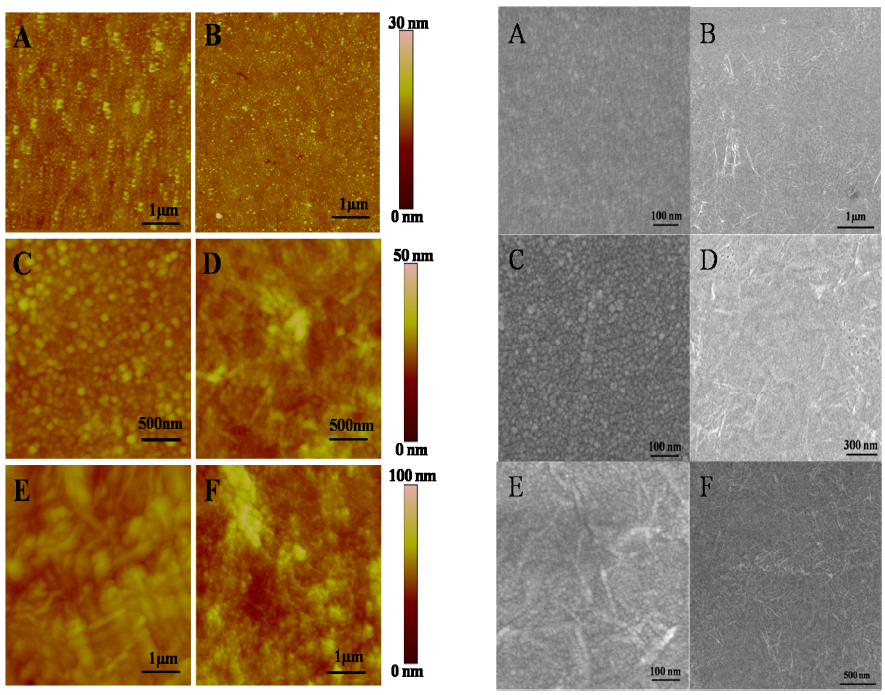


**Fig. S11** The AFM (left) and SEM (right) images of the composite films of $[PEI/P_5W_{30}]_1$ (A), $[PEI/P_5W_{30}/PEI/GO@F]_1$ (B), $[PEI/P_5W_{30}]_3$ (C), $[PEI/P_5W_{30}]_3[PEI/GO@F]$ (D), $[PEI/P_5W_{30}/PEI/GO@F]_3[PEI/P_5W_{30}]_1$ (E), $[PEI/P_5W_{30}/PEI/F@GO]_4$ (F).